Interaction of Rare Earth Chloride Salts to Alumina and Mullite in LiCl-KCl at 773 K

D. Horvath*, S. Warmann, J. King, K. Marsden, and R. Hoover
Idaho National Laboratory, 775 MK Simpson Blvd, Idaho Falls, ID83402, USA

Two commonly used ceramics in molten salt research are alumina and mullite. The two ceramics were exposed to a combination of rare earth chlorides (YCl_3, $SmCl_3$, $NdCl_3$, $PrCl_3$, and $CeCl_3$; each rare earth chloride of 1.8 weight percent) in LiCl-KCl at 773 K for approximately 13 days. Scanning electron microscopy with wave dispersion spectra was utilized to investigate a formation layer or deposition of rare earths onto the ceramic. Only the major constituents of the ceramics (Al, Si, and O_2) were observed during the wave dispersion spectra. X-ray fluorescence was used as well to determine concentration changes in the molten salt as a function of ceramic exposure time. This study shows no evidence of ionic exchange or layer formation between the ceramics and molten chloride salt mixture. There are signs of surface tension effects of molten salt moving out of the tantalum crucible into secondary containment.

Keywords: Molten salt, Ceramic, Ionic exchange, Rare earth chloride, Molten salt surface tension

*Corresponding Author.
David Horvath, Idaho National Laboratory, E-mail: david.horvath@inl.gov, Tel: +1-208-533-7957

ORCID

David Horvath	http://orcid.org/0000-0002-8171-1503	Stephen Warmann	http://orcid.org/0000-0002-5385-8794
James King	http://orcid.org/0000-0003-3728-4759	Kenneth Marsden	http://orcid.org/0000-0002-5366-7568
Robert Hoover	http://orcid.org/0000-0003-4715-6443		

Table 1. Thermodynamics of rare earth chlorides interacting with alumina and mullite

	T	ΔH	ΔS	ΔG
	℃	kcal	cal/K	kcal
$CeCl_3 + Al_2O_3 = Ce_2O_3 + AlCl_3$	500	138.7	31.5	114.3
$2CeCl_3 + 3Al_2O_3 = Ce_2O_3 + 6AlOCl$	500	118.6	-9.6	126.0
$2YCl_3(l) + Al_2O_3(s) = Y_2O_3(s) + 2AlCl_3(s)$	500	78.4	-5.6	82.7
$2YCl_3(l) + 3Al_2O_3(s) = Y_2O_3(s) + 6AlOCl(s)$	500	76.1	-8.6	82.8
$2SmCl_3(l) + Al_2O_3(s) = Sm_2O_3(s) + 2AlCl_3(s)$	500	101.6	-10.6	109.8
$2SmCl_3(l) + 3Al_2O_3(s) = Sm_2O_3(s) + 6AlOCl(s)$	500	99.3	-13.6	109.8
$2NdCl_3(l) + Al_2O_3(s) = Nd_2O_3(s) + 2AlCl_3(s)$	500	110.9	-10.0	118.6
$2NdCl_3(l) + 3Al_2O_3(s) = Nd_2O_3(s) + 6AlOCl(s)$	500	108.6	-13.0	118.6
$2PrCl_3(l) + Al_2O_3(s) = Pr_2O_3(s) + 2AlCl_3(s)$	500	116.7	-11.7	125.7
$2PrCl_3(l) + 3Al_2O_3(s) = Pr_2O_3(s) + 6AlOCl(s)$	500	114.4	-14.7	125.7

1. Introduction

Rare earth metals are widely used now in different fields of modern technologies when in high purity such as computer memory disks, rechargeable batteries, magnets, and fluorescent lighting. Electrowinning and electrorefining in molten salt are an option to manufacture high purity rare earth metals. Recycling of used nuclear fuel constitutes as another important technology related to rare earths and molten salts. This recycling is called pyroprocessing, and is a developing technology used in the nuclear fuel industry. The process operates at high temperature in a molten salt electrolyte. The goal is to recover actinides and minimize radioactive waste [1-8]. This is commonly referred to as electrorefining. The metallic fuel is dissolved anodically and the actinides are collected cathodically [9-16]. The salt in the electrorefiner (ER) contains most of the special nuclear materials. There is high interest to monitor the composition of this salt from an operational and safeguard perspective [17-21].

There are several options for monitoring the composition of the ER salt such as physical samples, in situ electrochemical sensors, and non-destructive assay. The reason for composition analysis is to ensure attractive material is not being removed from the ER as well as investigating corrosion of structure and operational equipment. These sensors are commonly developed on a bench scale experimental set up before deployment and are heavily impacted by analyte concentration. Such as electromagnetic forces will change if corrosion products are soluble in the ER salt [22-25].

Typically, the crucibles containing these molten chlorides are alumina crucibles [26-31]. Electrochemistry is a useful technique in molten salts to determine diffusion coefficients, activity coefficients, concentrations, and potentials. For electrical isolation of electrodes, ceramic tubes are used such as mullite. It is important to note these ceramics are Al_2O_3 (alumina) and a mixture of SiO_2 and Al_2O_3 (mullite) and may interact with the molten salts containing rare earth chlorides through ionic exchange to drawdown the concentration of rare earth chlorides. This work focuses on investigating the interaction of alumina and mullite between YCl_3, $SmCl_3$, $NdCl_3$, $PrCl_3$, and $CeCl_3$ in LiCl-KCl at 773 K.

The most likely interaction between the ceramics and

Table 2. Favorable conversation of rare earth chlorides to oxides or oxychlorides

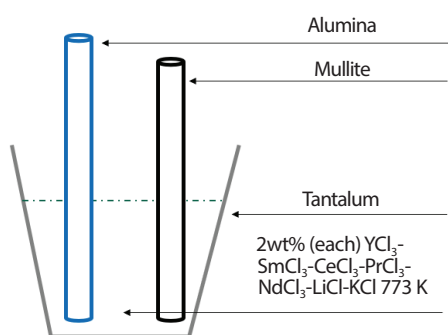|	Gibbs free energy (kcal/mole)	
	T (K)	
	723	823
$CeCl_3 + O_2(g) = CeO_2 + 3/2\ Cl_2$	-15.2	-15.9
$GdCl_3 + 1/2\ O_2(g) = GdOCl + Cl_2$	-4.3	-6.9
$NdCl_3 + 1/2\ O_2 = NdOCl + Cl_2$	-3.1	-3.7

Fig. 1. Tantalum crucible holding the molten salt chloride mixture containing alumina and mullite tubes at 773 K.
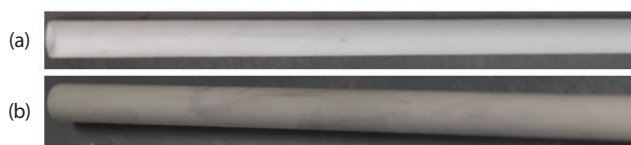

Fig. 2. (a) Alumina tube and (b) Mullite tube before exposure to the rare earth chloride salts at 773 K.

the salt would be an ionic exchange, such that the rare earth chloride would form a rare earth oxide or a rare earth oxychloride. A thermodynamic database HSC Chemistry 9 was used to evaluate the possibility of ceramic and salt interaction. Table 1 reveals possible chemical reactions.

The oxidation of these rare earth chlorides is possible when there is available free oxygen molecule. The change in free energy is favorable at 773 K [32]. The possibility of oxychlorides is also favorable when there is an available oxygen which could be removed from alumina and/or mullite. Table 2 presents thermodynamic values [32] from HSC 5.1.

Experimental: All electrochemical experiments were performed in an inert argon atmosphere glovebox (MBraun LABmaster dp). Conditions within the glovebox were maintained at less than 3 ppm O_2 and 1 ppm H_2O. No fluctuations in atmospheric concentrations were observed during the experiment. The salt mixture contained 24.6 g of LiCl-KCl eutectic (Sigma-Aldrich SAFC, anhydrous beads, 99.99%), 0.5 g of YCl_3 (99.99%, anhydrous, Sigma Aldrich), 0.5 g of $SmCl_3$ (99.9%, anhydrous, Sigma Aldrich), 0.5 g of $CeCl_3$ (>99.99%, anhydrous, Sigma Aldrich), 0.5 g of $PrCl_3$ (99.99%, anhydrous, Sigma Aldrich), and 0.5 g of $NdCl_3$ (>99.99%, anhydrous, Sigma Aldrich). The salt was contained in a tantalum crucible (99.9%, 20 ml Low Form, MTI Albany) which was then heated in a Kerr furnace to 773 K. Once at temperature, an alumina tube (5 inches, Open Ended, Advalue Tech) and mullite tube (5 inches, Open Ended, Coors Tech) were inserted approximately 0.5 inches into the molten salt. Fig. 1 presents the experimental set up within the Kerr Furnace.

After exposing the ceramics to the molten chloride mixture for approximately 13 days, the tubes were removed from the furnace and rinsed with tap water to remove any adhered salt; distilled water would have been preferred but was not currently available, any impurities in the tap water should not influence the purpose of these experiments. Approximately 11 mm was cut from the rod at the end immersed in the molten salt. For observation via a Scanning Electron Microscope (SEM) with Wavelength-Dispersive X-Ray Spectroscopy (WDS) the ceramic samples were ground and polished to achieve a 1-micron finish using Buehler discs and polishing suspensions.

2. Results and Discussion

Before the insertion of alumina and mullite to the molten chloride mixture, the tubes were weighed (6.30 and 8.20 g; alumina and mullite, respectively) and their surfaces documented. Fig. 2 shows photographs of the initial surfaces

Fig. 3. Ceramic tube alumina-above (a) and mullite-below (b) after immersion in YCl$_3$-SmCl$_3$-NdCl$_3$-PrCl$_3$- CeCl$_3$ in LiCl-KCl at 773 K.
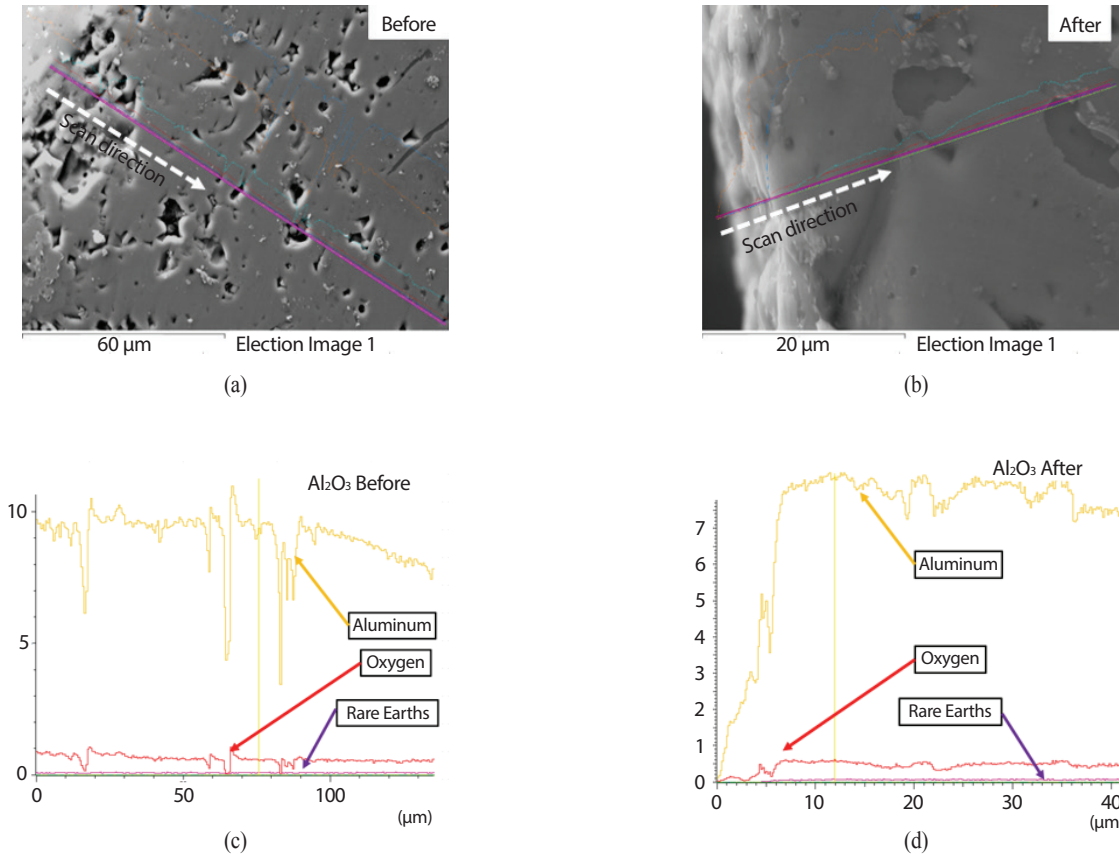

Fig. 4. Images of the alumina tube surface (a) before and (b) after immersion in rare earth chloride mixture at 773 K for 13 days (c) WDS of alumina before exposure to the rare earth chloride salt (d) WDS of alumina after direct exposure.

as received from the manufacturers and will be used as a visual comparison for any surface change.

After approximately 13 days of exposure to the salt, the ceramic tubes were removed from the furnace. Upon removal, several observations were made, the most noticeable is a surface discoloration as shown in Fig. 3. The portion of tube immersed in salt had darkened along with a slight discoloration at the top of the tube (still within the furnace). Due to the vapor pressure of these salts at 773 K,

it is possible that some salt vapors may have condensed on the cooler surfaces at the tops of the ceramic tubes. Interestingly, the middle portion of the tubes did not undergo major visual change, possibly due to the heat distribution of the tube within the furnace such that salt vapor preferentially deposited elsewhere. The ceramic tubes exhibited slight increases in mass following salt exposure and water rinse. The alumina tube increased by 2.5% to 6.46 g while the mullite mass increased by 1.1% to 8.29 g.
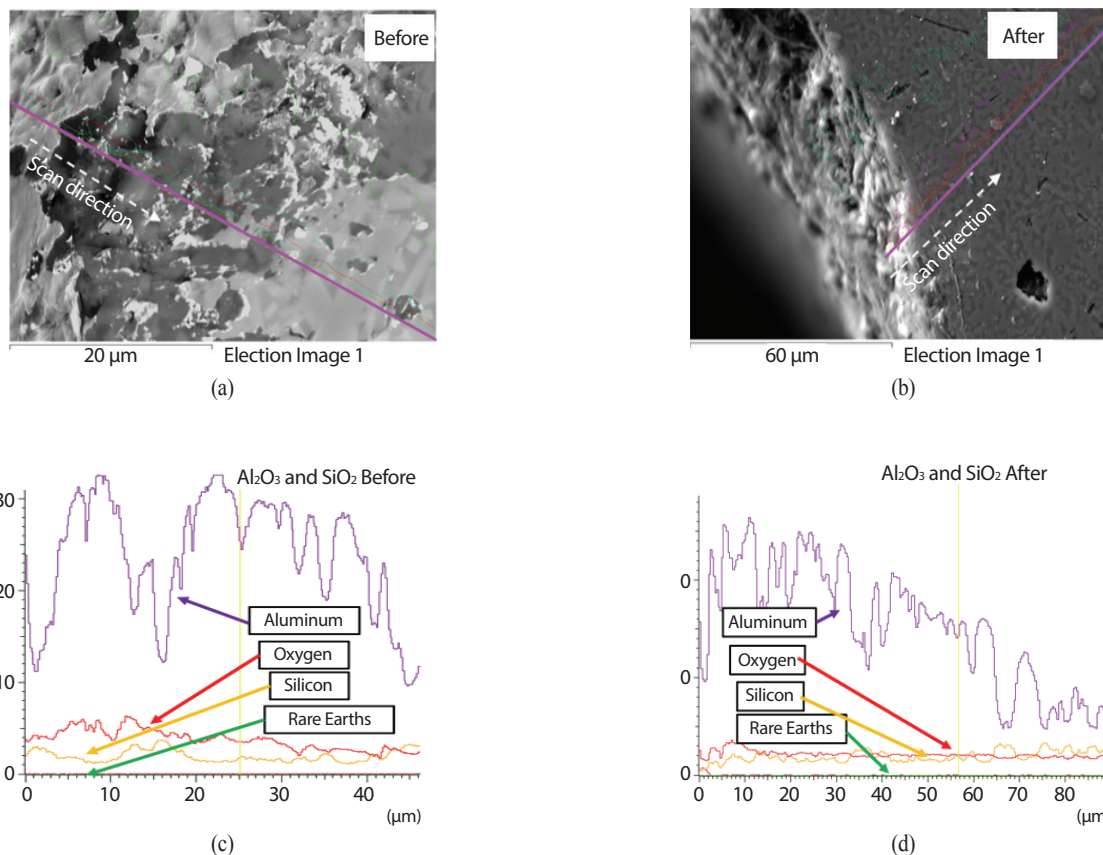
Fig. 5. Images of the mullite tube surface (a) before and (b) after immersion in rare earth chloride mixture at 773 K for 13 days (c) WDS of mullite before exposure to the molten salt mixture (d) WDS of mullite after 13 days of exposure to the molten salt mixture.

The tips of the exposed ceramic tubes exposed to the rare earth chloride salt were cut and prepared for observation via SEM (Oxford Instruments) with WDS (Inca wave) capabilities. The first ceramic to be viewed was Alumina. The initial image has a legend of 60 microns while the exposed surface was magnified further with a legend of 20 micron. The reason for additional magnification was to view the salt ceramic interface closer. Fig. 4(a) and 4(b) show a comparison before and after the rare earth chloride exposure of 13 days. Additionally, WDS was performed on the ceramic materials before and after the rare earth chloride exposure bath to investigate elemental differences. Alumina is a ceramic containing aluminum and oxygen (Al_2O_3) whereas mullite is a mixture of aluminum oxide and silicon oxide (SiO_2). Fig. 4(c) shows the WDS (before) and

Fig. 4(d) shows the WDS (after) the alumina was exposed to the rare earth chloride mixture for 13 days.

Comparing Fig. 4(c) and 4(d) there does not seem to be an ionically exchanged layer or trace of any rare earths on the surface and radially through the alumina. Fig. 5 shows the SEM images (a and b) and WDS results (c and d) for the mullite. Again, there does not appear to be any interaction at this magnification. The two most detectable elements were aluminum and oxygen, which are the primary components of the ceramic.

SEM comparisons provide crucial visual morphologic characteristics. For both cases (alumina and mullite) the surface appears to be visually similar in crevices and voids. Recall the discussion from the thermodynamic section, the SEM comparison verifies the thermodynamic calculations
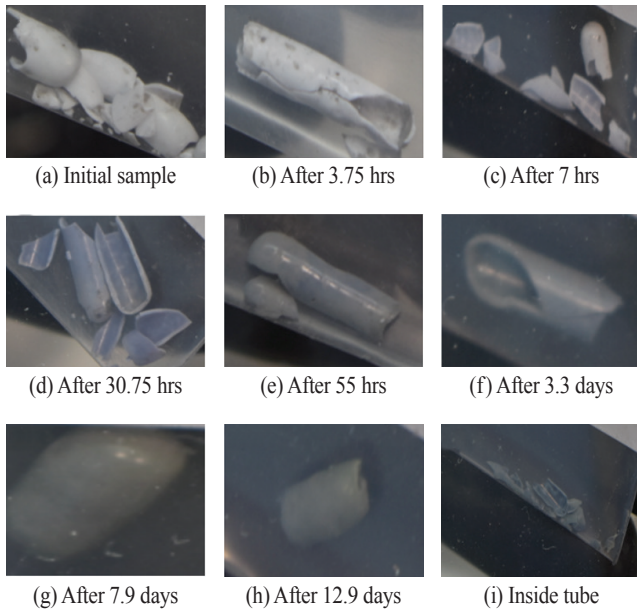
(a) Initial sample   (b) After 3.75 hrs   (c) After 7 hrs

(d) After 30.75 hrs   (e) After 55 hrs   (f) After 3.3 days

(g) After 7.9 days   (h) After 12.9 days   (i) Inside tube

Fig. 6. Salt samples taken during the alumina and mullite soak in
YCl_3-$SmCl_3$-$NdCl_3$-$PrCl_3$- $CeCl_3$- in LiCl-KCl at 773 K
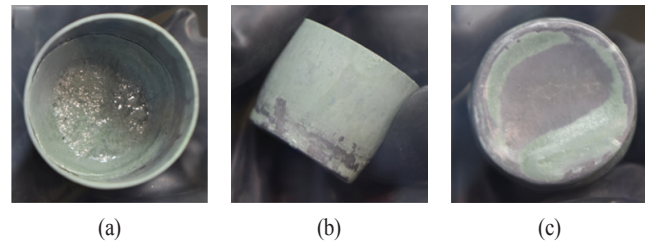as a function of time.

(a)   (b)   (c)

Fig. 7. Images of the (a) inside, (b) side, and (c) bottom of the tantalum
crucible containing the rare earth chlorides with alumina and mullite
tubes after 13 days.

Fig. 8. Frozen rare earth chloride salt puck that was deposited
underneath the tantalum crucible during the 13 days
of ceramic and salt mixture interaction.

which suggested no interaction would occur. It is important to note, at higher temperatures or different conditions the result may differ.

Throughout the 13-day period of exposure, samples were periodically taken of the salt, shown in Fig. 6. These samples aid in the visual detection of any changes occurred. Initially the salt mixture was white when frozen (translucent when liquid). After 7 hours of the ceramic being immersed in the rare earth chloride mixture; a blue hue began to appear. After roughly 8 days of ceramic exposure the blue hue began to change to a green color. Visual observation of the salt samples does not specify rare earth concentration or even that changes in the concentration have occurred. However, it is important to note the observed color changes may be due to an interaction with the surface of the ceramic tubes. Fig. 6 shows images of the salt samples taken as a function of exposure time. The last image within the figure represents the salt which was inside the tube at the end of 13 days.

After the experiment was concluded the tantalum crucible was removed from the furnace and a puck of salt was found below the crucible. Fig. 7 shows photographs of the inside, the side, and the underside of the tantalum crucible after the experiment. The movement of the molten salt at this temperature could be attributed to the wetting or surface tension between the molten salt and the ceramics and/or tantalum.

This frozen puck remaining in the furnace was easily removed from the graphite liner by turning the liner upside down. Fig. 8 shows photographs of the top, side, and bottom of the recovered salt. The weight of the frozen salt puck was 15.94 g. The bottom picture of the frozen puck shows a darkened region, which is graphite from the liner.

X-Ray Fluorescence (XRF) was performed on the salt samples to investigate concentration as a function of ceramic exposure time. It is important to note the accuracy associated with X-ray fluorescence; the machine used was from Malvern PANanalytical (Epsilon model) having a resolution of 135 eV at an elemental range of C-Am. Fig. 9 presents the concentrations determined from XRF, note
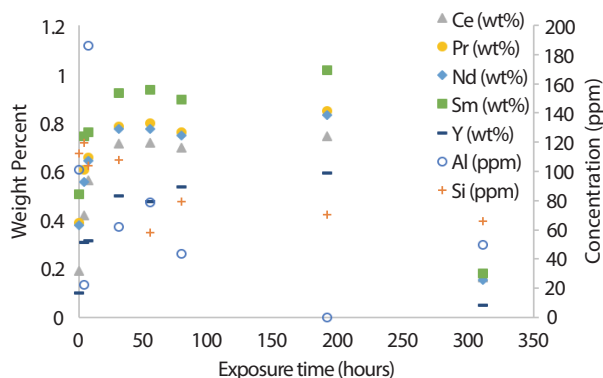
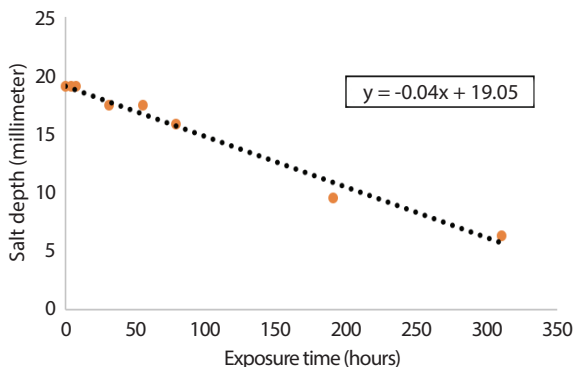Fig. 9. XRF results of the frozen salt samples.

Fig. 11. Molten chloride salt level as a function of time.
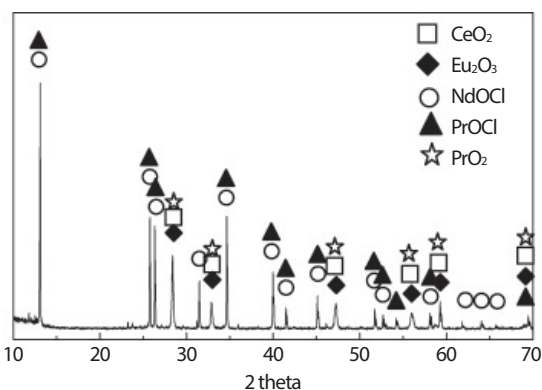

Fig. 10. XRD pattern of known rare earth oxides and oxychlorides [33].

Table 3. Comparison between the last salt sample taken versus the salt taken from inside the mullite tube

Element	310.75 hours wt%	Salt Inside Tube wt%
K	4.6	5.9
Y	0.05	0.08
Ce	0.2	0.2
Pr	0.2	0.3
Nd	0.2	0.2
Sm	0.2	0.3

Aluminum and Silicon are in units of parts per million (ppm). Inferring from the results, there does not appear to be a change in the rare earth concentration in the frozen salt

samples. It is true the weight percent values are less then expected but the XRF was not calibrated whereas ICP was calibrated using standard solutions. Lastly, a comparison of two salt samples was investigated; the last bulk sample taken was compared to a sample of the salt taken from inside the mullite tube. If there was a reaction to occur between the rare earth chloride salt and the ceramic tube, then the highest concentration difference should be inside the tube compared to outside the tube. Table 3 compares the concentrations found via XRF. The results between the two samples are similar, inferring no reaction occurred inside or outside the tube. It is important to note the XRF was calibrated for these elements. The main point was to observe if a difference in "relative" concentrations could be determined. However, the differences were observed.

Another piece of equipment which would accompany the XRF would be X-Ray Diffraction (XRD). XRD utilized the atomic structure of the crystal to scatter incoming x-rays to produce a unique pattern. Known patters of known crystals are placed into large databases so that unknown crystal structures being analyzed can be determined. A known pattern of rare earth oxides and oxychlorides have been published [33-34]. Fig. 10 could be compared with the samples generated if XRD was performed. This method would validate oxides or oxychloride formation on the surface with the ceramics.

Throughout the experiment there was a continual

change in salt depth. When each salt sample was taken, the salt level was simultaneously measured and is plotted as a function of time (Fig. 11). The mechanism for movement of the molten salt was not investigated, however the phenomena could possibly be attributed to the surface tension of the salt at the tantalum crucible surface or capillary effects.

It is evident the salt is moving out of the tantalum crucible. Recall, the salt is comprised of the rare earth chlorides and the eutectic LiCl-KCl. It is a possibility that the entire mixture is creeping up the tantalum, alumina, or mullite surface. This is analogous to a wetting effect. Further investigations could be performed between the tested surfaces and the components of the mixtures to determine a wetting angle. One such method is the Sessil drop method to determine the solid surface energies. A liquid drop is placed onto a flat surface, a contact angle can then be measured such that a higher repulsion will result in a higher contact angle. This is a relatively simple method but may be difficult when working with high temperature molten salts. It would be difficult to incorporate a transparent window into the vessel at these high temperatures.

3. Conclusions

Molten salts are gaining popularity in a variety of fields such as heat transfer fluids, thermal batteries, solvents, and coolant or fuel in molten salt reactors. As experiments and investigations are conducted in molten salts, it is important to understand the effects of the materials containing these salts. There could be possible interactions such as ionic exchange, galvanic corrosion, and other interactions which may affect the purity of these salts, which also impacts the conclusion of the experiments. This work sought to determine the interaction of alumina and mullite, which are commonly used to contain molten LiCl-KCl, at 773 K with a nominal concentration of around 9 weight percent rare earth chlorides. After 13 days of exposure to this salt the ceramics and collected

salt samples showed visual changes. Intuitively, this color change would suggest an interaction between the ceramics and the salt. However, after viewing the ceramic under a scanning electron microscope with wave dispersion spectra capabilities, no interactions were observed. If a film were to have formed from ionic interaction or by other means, it was not observed in the prepared samples. An interesting phenomenon occurred during the experiment such that majority of the molten salt did not remain inside the tantalum crucible. Instead, the molten salt covered the outside of the crucible and deposited on the graphite furnace liner. This may be due to a higher than expected surface tension of this specific salt mixture and/or an interaction between the salt and the tantalum crucible or ceramic tubes.

REFERENCES

[1] J.J. Laidler, J.E. Battles, W.E. Miller, J.P. Ackerman, and E.L. Carls, "Development of Pyroprocessing Technology", Prog. Nucl. Energy., 31, 131-140 (1997).

[2] E.Y. Choi and S.M. Jeong, "Electrochemical Processing of Spent Nuclear Fuels: An Overview of Oxide Reduction in Pyroprocessing Technology", Pro. Nat. Sci., 25, 572-582 (2015).

[3] H.S. Lee, G.I. Park, K.H. Kang, J.M. Hur, J.G. Kim, and E.H. Kim, "Pyroprocessing Technology Development at KAERI", Nucl. Eng. Technol., 43, 317-328

(2011).

[4] H. Lee, G.I. Park, J.W. Lee, K.H. Kang, J.M. Hur, and I.J. Cho, "Current Status of Pyroprocessing Development at KAERI", Sci. Technol. Nucl. Ins., 2013 (2013).

[5] J.H. Yoo, C.S. Seo, E.H. Kim, and H.S. Lee, "A Conceptual Study of Pyroprocessing for Recovering Actinides from Spent Oxide Fuels", Nucl. Eng. Technol., 40, 581-592 (2008).

[6] H. Ohta, T. Inoue, Y. Sakamura, and K. Kinoshita, "Pyroprocessing of Light Water Reactor Spent Fuels Based on a Electrochemical Reduction Technology", Nucl. Technol., 150, 153-161 (2005).

[7] K. Nagarajan, B.P. Reddy, S. Ghosh, G. Ravisankar, K.S. Mohandas, and P.V. Rao, "Development of Pyrochemical Reprocessing for Spent Metal Fuels", Energy Procedia, 7, 431-436 (2011).

[8] T. Satoh, T. Iwai, and Y. Arai, "Electrolysis of Burnup-Simulated Uranium Nitride Fuels in LiCl-KCl Eutectic Melts", J. Nucl. Sci. Technol., 6, 557-563 (2009).

[9] S. Li, X. Sofu, T. Johnson, and D.V. Laug, "Experimental Observations on Electrorefining Spent Nuclear Fuel in Molten LiCl-KCl/liquid Cadmium System", J. New Mat. Electrochem. Sys., 3, 259-268 (2000).

[10] T. Kobayashi, R. Fujita, M. Fujie, and T. Koyama, "Polarization Effects in the Molten Salt Electrorefining of Spent Nuclear Fuel", J. Nucl. Sci. Technol., 32, 653-663 (1995).

[11] C.C. McPheeters, E.C. Gay, E.J. Karell, and J.P. Ackerman, "Electrometallurgically Treated Metal, Oxide and Al Alloy Spent Nuclear Fuel Types", J. Mater., 49, 22-25 (1997).

[12] S.X. Li, T.A. Johnson, B.R. Westphal, K.M. Goff, and R.W. Benedict, "Electrorefining Experience for Pyrochemical Reprocessing of Spent EBR-II Driver Fuel", Proc. of Global 2005, INL/CON-05-00305, October 9-13, 2005, Tsukuba, Japan.

[13] R.G. Lewin and M.T. Harrision, "International Developments in Electrorefining Technologies for Pyrochemical Processing of Spent Nuclear Fuels", Reproc.

Recycl. Spent Nucl. Fuel, 1, 373-413 (2015).

[14] T. Koyama, R. Fujita, M. Hzuka, and Y. Sumida, "Pyrometallurgical Reprocessing of Fast Reactor Metallic Fuel-Development of a New Electrorefiner with a Ceramic Partition", Nucl. Technol., 110, 357-368 (1995).

[15] J.H. Lee, Y.H. Kang, S.C. Hwang, E.H. Yoo, and H.S. Park, "Separation Characteristics of a Spent Fuel Surrogate in the molten Salt Electrorefining Process", J. Mater. Process Technol., 189, 268-272 (2007).

[16] P. Soucek, T. Murakami, B. Claux, R. Meier, R. Malmbeck, and J.P. Glatz, "Separation of Actinides from Irradiated An-Zr Based Fuel by Electrorefining on Solid Aluminum Cathodes in Molten LiCl-KCl", J. Nucl. Mater., 459, 114-121 (2015).

[17] K.M. Goff, J.C. Wass, K.C. Marsden, and G.M. Teske, "Electrochemical Processing of Used Nuclear Fuel", Nucl. Eng. Technol., 43, 335-342 (2011).

[18] H.E. Garcia, M.J. Lineberry, S.E. Aumeier, and H.F. McFarlane, "Proliferation Resistance of Advanced Sustainable Nuclear Fuel Cycles", Nucl. Plant J., 20, 18-27 (2002).

[19] W. Zhou, Y. Wang, and J. Zhang, "Integrated Model Development for Safeguarding Pyroprocessing Facility: Part II-Case Studies and Models Integrations", Ann. Nucl. Energy, 112, 48-61 (2018).

[20] K.M. Goff, R.D. Mariani, D. Vaden, N.L. Bonomo, and S.S. Cunningham, "Fuel Conditioning Facility Electrorefiner Start-Up Results", Proc. of the 1996 Annual meeting of the American Nuclear Society, ANL--TD/CP-89649, June 16-20, 1996, Reno, United States.

[21] T.Y. Gutnecht, G.L. Fredrickson, and V. Utgikar. Thermal Analysis of Surrogate Simulated Molten Salts with Metal Chloride Impurities for Electrorefining Used Nuclear Fuel, Idaho National Laboratory Technical Report, INL/EXT-11-23511 (2012).

[22] H.A. Laitinen and C.H. Liu, "An Electromotive Force Series in Molten Lithium Chloride-Potassium Chloride Eutectic", J. Am. Chem. Soc., 80(5) , 1015-1020

(1958).

[23] Y. Sakamura, T. Hijikata, K. Kinoshita, T. Inoue, T.S. Storvick, C.L. Krueger, and R.L. Gay, "Measurement of Standard Potentials of Actinides (U, Np, Pu, Am) in LiCl-KCl Eutectic Salt and Separation of Actinides from Rare Earths by Electrorefining", J. Alloys Compd., 271, 592-596 (1998).

[24] S.A. Slater, A.G. Raraz, J.L. Willit, and E.C. Gay, "Electrochemical Separation of Aluminum from Uranium for Research Reactor Spent Nuclear Fuel Applications", Sep. Purif. Technol., 15, 197-205 (1999).

[25] A.V. Novoselova and V.V. Smolenskii, "Electrochemical and Thermodynamic Properties of Lanthanides (Nd, Sm, Eu, Tm, Yb) in Alkali Metal Chloride Metals", Radiochemistry, 55, 243-256 (2013).

[26] S.A. Kuznetsov and M. Gaune-Escard, "Electrochemical Transient Techniques for Study of the Electrochemistry and Thermodynamics of Nuclear Materials in Molten Salts", J. Nucl. Mater., 15, 108-114 (2009).

[27] A.R. Shankar and U.K. Mudali, "Corrosion of Type 316L Stainless Steel in Molten LiCl-KCl Salt", Mater. Corros., 59, 878-882 (2008).

[28] J.H. Sim, Y.S. Kim, and I.J. Cho, "Corrosion Behavior Induced by LiCl-KCl in Type 304 and 316 Stainless Steel and Copper at Low Temperature", Nucl. Eng. Technol., 49, 769-775 (2017).

[29] M. Hofmeister, L. Klein, H. Miran, R. Rettig, S. Virtanes, and R.F. Singer, "Corrosion Behavior of Stainless Steels and a Single Crystal Superalloy in a Ternary LiCl-KCl-CsCl Molten Salt", Corros. Sci., 90, 46-53 (2015).

[30] A.R. Shankar, U.K. Mudali, R. Sole, H.S. Khatak, and B. Raj, "Plasma-Sprayed Yttria-Stabilized Zirconia Coatings on Type 316L Stainless Steel for Pyrochemical Reprocessing Plant", J. Nucl. Mater., 372, 226-232 (2008).

[31] A.R. Shankar, K. Thyagarajan, and U.K. Mudali, "Corrosion Behavior of Candidate Materials in Molten LiCl-KCl Salt Under Argon Atmosphere", Corrosion, 69(7), 655-665 (2013).

[32] H. C. Eun, Y.Z. Cho, H.S. Park, T.K. Lee, I.T. Kim, K.I. Park, and H.S. Lee, "Study on a Recovery of Rare Earth Oxides from a LiCl-KCl-RECl₃ System", J. Nucl. Mater., 1, 110-115 (2011).

[33] H.C. Eun, H.C. Yang, Y.Z. Cho, H.S. Lee, and I.T. Kim, "Vacuum Distillation of a mixture of LiCl-KCl Eutectic Salts and RE Oxidation Precipitates and a Dechlorination of RE Oxychlorides", J. Hazard. Mater., 160, 634-637 (2008).

[34] Y.Z. Cho, H.C. Yang, G.H. Park, H.S. Lee, and I.T. Kim, "Treatment of a Waste Salt Delivered from an Electrorefining Process by an Oxidative Precipitation of the Rare Earth Elements", J. Nucl. Mater., 3, 256-261 (2009).